physica status solidi a
www.pss-a.com

Integration of PEDOT:PSS into Cotton Yarn as Ion-Selective Sensors for Smart Clothing Applications

*Chunling Li, Ni Zhang, Sven Ingebrandt, and Xuan Thang Vu**

In recent years, textile sensors have played a crucial role in the development of smart clothing, which integrates electronic components and technology into garments. Furthermore, a variety of textile sensors in smart clothing have gained attention for their healthcare applications, including analyzing sweat, monitoring biomarkers, and sensing electrophysiology. The conductive polymer poly (3,4-ethylene dioxythiophene): polystyrene sulfonate (PEDOT:PSS) has been explored for various applications, such as flexible and wearable electronics, neural interfaces, and bioelectronics devices. Herein, a sensitive and selective ion detection utilizing cotton yarn-based textile sensors integrated with ion-selective membranes (ISMs) is presented. First, a straightforward and reproducible approach for manufacturing textile sensors based on PEDOT:PSS is described. The relationship between the resistance change of these sensors and their performance, encompassing stability and flexibility is investigated. Following this, ISMs are integrated into the sensors to detect sodium (Na^+) and potassium (K^+) ions, separately. The sensors display a consistent linear response toward the detected ion in a concentration range from 1 to 50 mM. Moreover, the sensors exhibit notable selectivity against the undesired ion.

1. Introduction

In recent years, the emergence of novel processing technologies and the expansion of textile sensors capabilities have strongly advanced in the application of smart clothing.[1] Due to their intrinsic properties of comfortability, flexibility, and breathability, textile sensors play a significant role in various healthcare applications.[2] In the near future, several textile sensor innovations are expected to be available for commercial use in the medical and sports industries.[1] Especially, smart socks, shirts, and gloves provide wearable solutions for monitoring crucial health indicators such as blood pressure, skin temperature, and hydration status.[1,3] Moreover, textile sensors serve as a highly effective tool for real-time and noninvasive monitoring of numerous biological parameters, like glucose levels,[4–6] ion concentrations,[7,8] and pH changes.[7,9] By detecting specific ions and biologically relevant molecules, textile sensors play a crucial role in the essential mission of monitoring and evaluating health parameters. This highlights their profound significance in this crucial context.

Ions are highly abundant in diverse natural environments, found within living organisms, and exist in various biofluids.[10–12] For example, the detailed physiological data and essential biomarkers found in sweat provide valuable insights into health conditions.[13–16] The concentration of sodium ions (Na^+) serves as a useful biomarker for identifying and assessing electrolyte imbalances.[17,18] Excessive loss of sodium (e.g., during sports activities) can cause serious health problems, for instance, hyponatremia and dehydration.[19] The concentration of potassium ions (K^+) is an essential biomarker to maintain body fluid balance, acid–base balance, and the regulation of body processes.[10] A low K^+ concentration can lead to hypokalemia, increasing the risk of high blood pressure and stroke.[20] Therefore, there is a substantial demand to accurately measure the concentration of sodium and potassium ion in sweat. Furthermore, because of its easy accessibility and noninvasive sample collection, ion detection in sweat is widely acknowledged as a critical choice for biosensing applications.[21–24]

Over the recent years, poly (3,4-ethylenedioxythiophene): poly(styrenesulfonic acid) (PEDOT:PSS) has gained significant research attention,[25–27] owing to its outstanding attributes such as high electrical conductivity, transparency, flexibility, and biocompatibility.[28–30] PEDOT:PSS is a hole-conducting organic semiconductor, which provides both ionic and electronic conductivity.[31] PEDOT:PSS is commonly integrated into organic electrochemical transistors (OECTs) with a three-terminal configuration: source, drain, and gate. This configuration makes PEDOT:PSS OECTs highly promising for a wide range of biosensing applications. By applying the gate voltage, the doping state of PEDOT:PSS can be controlled by introducing or removing ions from the surrounding electrolyte solution into the polymeric film. As a result, this alteration has a notable effect on the electric conductivity of PEDOT:PSS, leading to the change in drain current of the OECTs. Additionally, PEDOT:PSS can also

C. Li, N. Zhang, S. Ingebrandt, X. T. Vu
Institute of Materials in Electrical Engineering 1
RWTH Aachen University
Sommerfeldstr. 24, Aachen 52074, Germany
E-mail: vu@iwe1.rwth-aachen.de

The ORCID identification number(s) for the author(s) of this article can be found under https://doi.org/10.1002/pssa.202400086.

DOI: 10.1002/pssa.202400086

be integrated into sensors with a two-terminal configuration, which is typically cost-effective and easily accessible. The integration of PEDOT:PSS into two-terminal sensors extends its utility to diverse applications, including pH changes tracking,[7] humidity monitoring,[32] and gas sensing.[33]

Appling conductive coatings or incorporating conductive polymers into textiles represents a widely adopted approach in the manufacturing of textile sensors.[34,35] PEDOT:PSS has been incorporated into textiles, including cotton yarn and nylon, resulting in distinct textile-integrated sensors.[36–38] Due to its ion conductive properties, PEDOT:PSS textile sensors are sensitive to the changes in ionic strength of analyte, making them highly adaptable for detecting a wide range of ions.[39] However, a significant challenge for PEDOT:PSS textile sensors is to achieve the selectivity toward specific ions, as all cations from the electrolyte can be diffused into the PEDOT:PSS channel during the gating.[40] To overcome this limitation, ion-selective membranes (ISMs) can be integrated onto the textile sensors for specific ion detection and monitoring.[41–43]

In this work, we report the sensitive and selective ions detection by employing two-terminal PEDOT:PSS textile sensors integrated with ISMs. First, the manufacturing process of PEDOT:PSS textile sensors based on cotton yarn is presented. Furthermore, the correlation between the resistance of the textile sensors and varied immersion times into the PEDOT:PSS solution during fabrication is investigated. Subsequently, the performance of the textile sensors is studied, including stability and flexibility. Finally, the textile sensors integrated with ISMs are utilized to detect various ions.

2. Experimental Section

2.1. Chemicals

PEDOT:PSS solution (Clevios PH 1000) was purchased from Heraeus, Germany. Ethylene glycol (EG), 3-Glycidyloxypropyltriethoxysilan (GOPS), sodium phosphate dibasic (Na_2HPO_4), sodium phosphate monobasic (NaH_2PO_4), potassium phosphate dibasic (K_2HPO_4), potassium phosphate monobasic (KH_2PO_4), Na ionophore X, sodium tetrakis [3, 5 bis (trifluoromethyl) phenyl] borate (Na-TFPB), polyvinyl chloride (PVC), bis (2-ethylhexyl) sebacate (DOS), tetrahydrofuran, kalium-ionophore III (valinomycin), and kalium-tetrakis-(4-chlorphenyl)-borat (KTB) were all procured from Sigma-Aldrich, Taufkirchen, Germany.

2.2. Preparation of PEDOT:PSS Solution, ISM Solutions and Buffer Solutions

2.2.1. PEDOT:PSS Solution

First, PEDOT:PSS solution was filtered using a 200 nm syringe filter (Luer Solo, B.Braun Melsungen AG, Germany) to remove the bigger particles. The filtered PEDOT:PSS solution was then mixed with EG and GOPS in a ratio of 500:25:4 v/v to obtain a PEDOT:PSS mixed solution.[44,45] The addition of EG and GOPS has been shown to enhance the electrical conductivity and the stability of PEDOT:PSS thin films in aqueous solution.[12]

2.2.2. ISM Solutions

The Na^+ selective membrane mixture was composed of Na ionophore X, Na-TFPB, PVC, and DOS in the ratio of 1:0.55:33:65.45 (w/w, 100 mg).[18,46] Then, 100 mg of the mixture was dissolved in 660 µL of THF with shaking for 10 min until getting a transparent membrane solution. Similarly, the K^+ selective membrane mixture consisting of Kalium-ionophore III, KTB, PVC, and DOS in the ratio of 2:0.5:32.7:64.7 (w/w) was prepared. An amount of this mixture was dissolved in 660 µL of THF with thoroughly mixing for 10 min to obtain a homogenous membrane solution.[18,46] Both ISM solutions were sealed and stored at 4 °C without light when not in use.

2.2.3. Buffer Solutions

The sodium buffer solutions were obtained by mixing Na_2HPO_4 and NaH_2PO_4 solutions, while the potassium buffer solutions were similarly prepared with mixing K_2HPO_4 and KH_2PO_4 solution. The pH value of 7 and the concentrations (1, 5, 10, and 50 mM) of all buffer solutions were controlled using a pH and conductivity meter (HI5522, Hanna Instruments Deutschland GmbH, Vöhringen, Germany). The 50 mM buffer solutions were diluted with deionized (DI) water to obtain lower concentrations of buffer solutions.

2.3. Preparation of Textile Sensors with ISMs

2.3.1. Materials

The cotton yarn utilized in this work is commercially available in commercial market (17.HIN.13 831, Søstrene Grene, Germany). Metal wires with a length of 10 cm were used (TW-MP-10, Twin Industries, Germany). Additionally, curing adhesive silver glue (No. T1312109, Kemo Electronic GmbH, Germany) was used, which effectively bonds at low temperatures. The silicone adhesive (No. 96-083, Dow Silica, United States) consisting of a base component A and a curing agent B was used. When A and B components were mixed in a ratio of 10:1 (w/w) and then exposed to heat, the silicone adhesive cured and gained its adhesive properties.

2.3.2. Fabrication Process

The primary fabrication process of the textile sensor is displayed in **Figure 1**a. The cotton yarn was first cleaned using DI water and then precisely trimmed to a length of 1.5 cm, while maintaining a uniform diameter of 0.6 mm. Then, the cotton yarn was immersed in a PEDOT:PSS solution with the immersing time ranging from 2 to 12 s (Figure 1b). Then, the PEDOT:PSS-coated cotton yarn was carefully transferred to an oven preheated to 80 °C, where it remained for 1 h.

Afterward, the cotton yarns coated with PEDOT:PSS were connected with the metal wires using silver glue and then dried at room temperature in the air. To insulate the connection points of the wire and cotton yarn from the surrounding air or solution, a layer of silicone adhesive was applied. Following that, the samples were carefully placed in an oven and dried at 50 °C for 24 h to obtain the textile sensors.

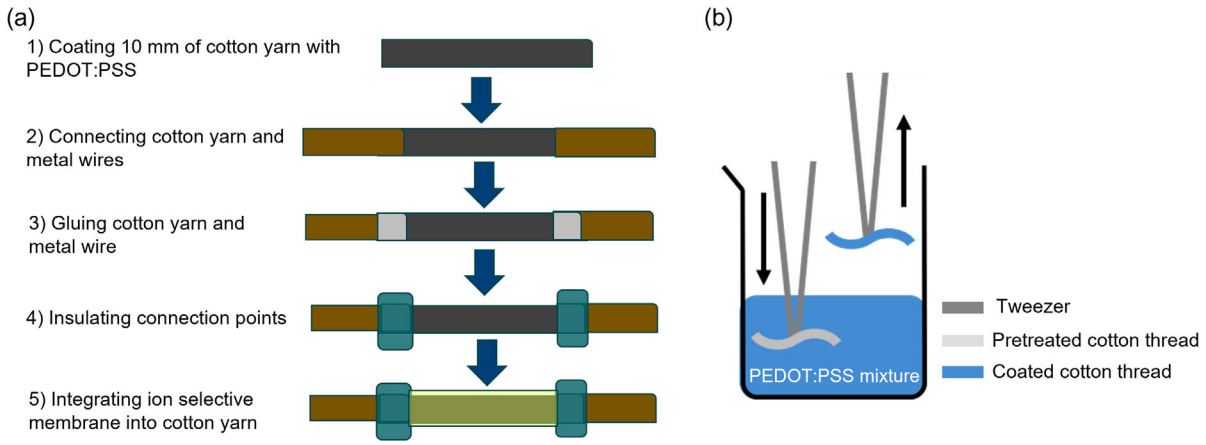

Figure 1. a) Schematics of the fabrication process of the textile sensors integrated with ISMs: step1: coating 10 mm of cotton yarn with PEDOT:PSS, step2: connecting the cotton yarn and the metal wire, step3: gluing cotton yarn with metal wires using silver glue, step4: insulating the connection points using the silicon adhesive, and step5: integrating the ISM into the cotton yarn. b) Schematics of the PEDOT:PSS coating process on the cotton yarn.

In the process of fabricating textile sensors integrated with ISMs, the initial step was submerging PEDOT:PSS-coated cotton yarns into an ISM solution for 10 s. Subsequently, the textile sensors were air-dried for 10 min.

2.4. Electrical Characteristics of the Textile Sensors

The two-probe resistance measurement technique was used to characterize the resistance of the fabricated textile sensors in the air and in different buffer solutions. The electrical characteristics were facilitated by the use of a semiconductor characterization system (4200 A-SCS, Keithley instruments, USA). The voltage sweep ranging from -0.1 to $+0.1$ V was systematically applied to the two ends of the textile sensors. The resulting resistance was determined by calculating the slope of the linear I–V curve through the formula $R = V/I$, where V and I represent the applied voltage and the measured current value, respectively.

3. Results and Discussion

3.1. Microscopic Characteristics of Textile Sensors Covered with ISMs

The textile sensors based on PEDOT:PSS for ion detection are shown in **Figure 2**. As shown in Figure 2a, PEDOT:PSS was uniformly integrated into the cotton yarn, indicating the homogeneity in the blue color of the yarn. The cotton yarn coated with PEDOT:PSS had a length of ≈10 mm. The two ends of the yarn were connected with metal wires using silver glue, as mentioned in Section 2.3. These connection points between the yarn and metal wire were completely covered with the silicon adhesive to provide an effective insulation for the connection points that are exposed to the measurement solutions in our experiments as well.

An ISM was integrated on the sensors by immersing the cotton yarn-coated PEDOT:PSS into the respective membrane solution for 10 s and dried in air at room temperature. Figure 2b shows a textile sensor covered with a selective membrane for the detection of potassium ions. The cotton yarn of this textile sensor displays a uniform and distinctive yellow color, resulting from the incorporation of the potassium ISM solution with yellow color. Similarly, the textile sensor integrated with a sodium ISM was fabricated using the identical procedure. The images in Figure 2 display typical examples of the straightforward and highly reproducible fabrication process for textile sensors integrated with ISMs.

3.2. Electrical and Electrochemical Characteristics of the PEDOT:PSS-Based Textile Sensors

The electrical characterization of the fabricated textile sensors was carried out in air. The current–voltage (I–V) characteristics

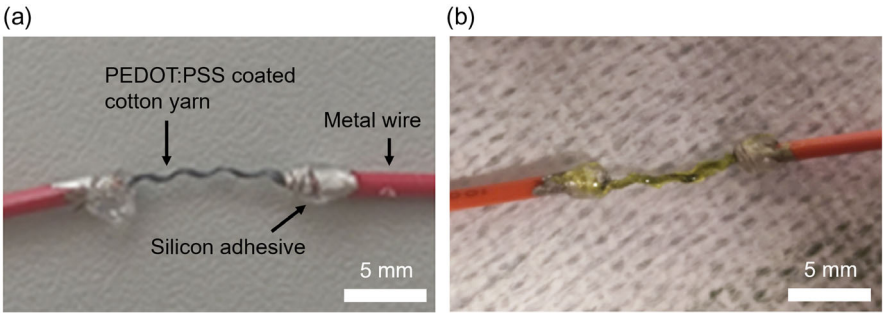

Figure 2. a) Images of a textile sensor before and b) after integrating it with a potassium ISM.

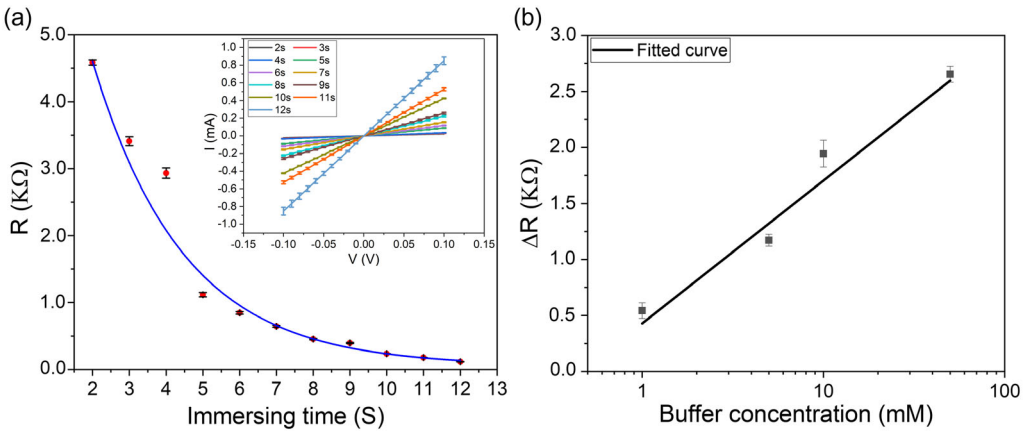

Figure 3. a) Resistance of the textile sensors fabricated with different immersing times in PEDOT:PSS solution and the *I–V* curves of textile sensors are in subfigure ($n = 3$); b) after fabricating the textile sensors using an immersing time of 4 s in PEDOT:PSS solution, the resistance change (ΔR) of these textile sensors was measured in buffer solutions with varying concentrations ($n = 3$).

of the sensors were performed by sweeping the voltage from −0.1 to +0.1 V. As shown in the subfigure of **Figure 3**a, the *I–V* characteristics of the fabricated textile sensors exhibit a linear behavior. Figure 3a presents the resistance of the textile sensors after coating the cotton yarn with PEDOT:PSS for various immersing times ranging from 2 to 12 s. For each immersion time, three sensors were fabricated. Results are displayed as mean values and small error bars indicate the highly reproducible fabrication process. Moreover, the results show that the resistance of those sensors decreases with increasing the immersing time. The decrease in the resistance follows an exponential relationship with the immersing time. This exponential relationship can be explained by the combined mechanisms of liquid diffusion[47] and wetting effects.[48,49]

Furthermore, we investigated the electrochemical characteristics of textile sensors by analyzing the changes of resistance in sodium buffer solutions with varying concentrations (1, 5, 10, and 50 mM). First, the *I–V* characteristics of three sensors were carried out in DI water, which served as a reference data point for the analysis of the resistance change in different buffer solutions. The textile sensors were then submerged in sodium buffer solutions (pH = 7) with concentrations ranging from low to high (1–50 mM). The *I–V* characteristics were measured after 10 s of submersion. In Figure 3b, the resistance changes (ΔR) of the textile sensor, which were all fabricated with the immersion time of 4 s in PEDOT:PSS solution, are displayed. The calculation was performed using the formula $\Delta R = R - R_0$, where R and R_0 were the resistance value obtained in buffer solution and DI water, respectively. As expected from the electrochemical characteristics of PEDOT:PSS, an increase in resistance was observed with an increase in buffer concentration. The resistance changes of the textile sensor show a linear relationship with the buffer concentrations on a logarithmic scale within our measured concentration range. As the textile sensor was submerged in the buffer solution, cations can diffuse into the PEDOT:PSS-coated cotton yarn, leading to the de-doping of the PEDOT:PSS according to the following equation

$$\mathrm{PEDOT^+: PSS^-} + M^+ + e^- \leftrightarrow \mathrm{PEDOT} + M^+\mathrm{: PSS^-} \quad (1)$$

where M^+ represents the cations. This mechanism leads to a reduction in available charge carriers in PEDOT, resulting in a decrease in conductivity of PEDOT:PSS. As a result, the resistance of textile sensors increases, which is consistent with this theoretical framework. Furthermore, this electrochemical characteristics of the PEDOT:PSS-based textile sensors validate the functionality of our textile sensors as electrochemical sensors.

3.3. Stability and Flexibility of the Textile Sensors

We tested the long-term stability of the textile sensors by evaluating the resistance on different days after the fabrication. As a standard characterization method, the *I–V* characteristics of the sensors were measured in dry condition and the resistance values were calculated from the *I–V* characteristics. Once the fabrication was finished, the initial resistance of the textile sensor was recorded. Subsequently, the sensors were exposed to the air for a specific day. Afterward, the resistance was re-evaluated on a daily base and compared to its initial resistance taken on the day of fabrication. For each data point, three sensors were measured and their average resistance values are presented. In **Figure 4**a, the stability of the textile sensors, which were immersed in PEDOT:PSS solution for 2 (black), 3 (red), and 4 s (blue), is displayed. All curves shown in Figure 4a exhibit stable resistance values with negligible fluctuations throughout the observation period, indicating that the textile sensors maintain their stability in the air for up to 5 d.

The flexibility of the textile sensors in the air was assessed by measuring the resistance changes resulting while bending the cotton yarn of the textile sensors at 5 distinct angles (0°, 45°, 90°, 135°, and 180°). The resistance of the textile sensor was measured three times at each bend angle to obtain an average resistance for each data point. In Figure 4b, the resistance values of the textile sensors, which were immersed in PEDOT:PSS solution for 2 (black), 3 (red), and 4 s (blue), are respectively presented after undergoing bending at different angles. The resistance values of these textile sensors exhibit remarkable stability when subjected to varying degrees of bending. The consistently observed results provide convincing proof that the structural integrity of the PEDOT:PSS coating on the cotton yarn remained intact under bending. The results of this

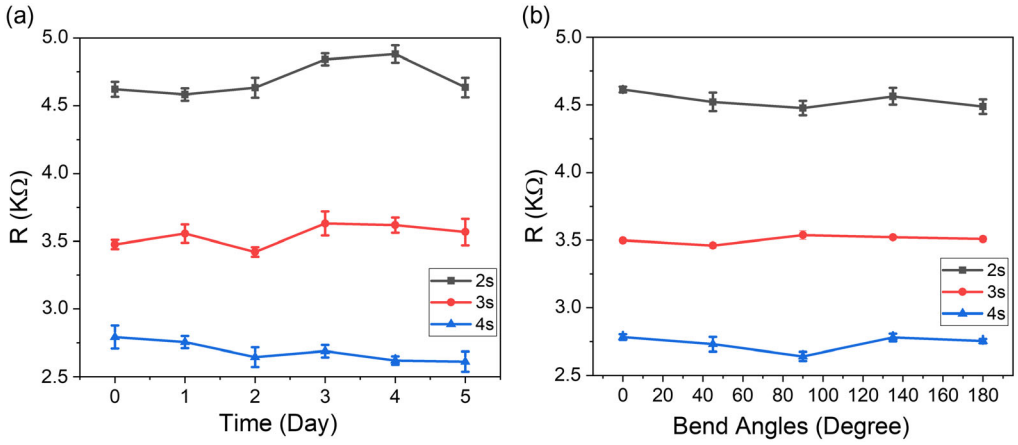

Figure 4. a) Resistance values of the sensors at different days with 2 (black), 3 (red), and 4 s (blue) of immersing times in PEDOT:PSS solution during fabrication ($n = 3$); b) resistance of the sensors at various bending angles with different immersing times ($n = 3$).

characterization demonstrate the potential for the application of our PEDOT:PSS textile sensors in flexible and wearable scenarios.

3.4. Ion Detection-Based on Textile Sensors

We integrated sodium ISMs (Na ISMs) and potassium ISMs (K ISMs) onto the textile sensors, respectively, to investigate the ion detection. The integration of the ISM onto the sensors involved immersing the cotton yarn coated with PEDOT:PSS into the membrane solution for 10 s, and then drying in air at room temperature. **Figure 5**a shows the measurement setup for ion detection using the ISM textile sensors. The ISM textile sensors were immersed into various solutions, and connected to the semiconductor characterization system to conduct the *I*–*V* characteristics. The voltage range of −0.1 to +0.1 V was applied after 10 s of submerging the ISM textile sensors in the solutions, and

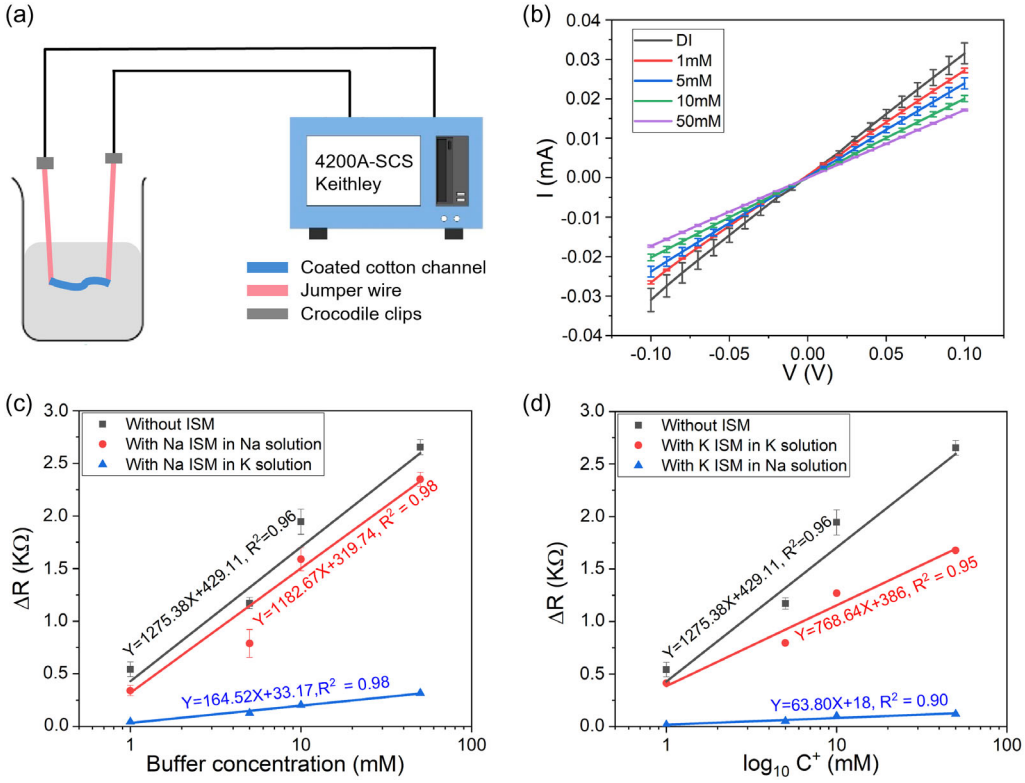

Figure 5. a) Measurement procedure for the ion detection using ISM-coated textile sensors; b) *I*–*V* characterization for sodium ion detection in sodium buffer solutions utilizing the sodium ISM textile sensors with 4 s of immersing time ($n = 3$); c) when the immersing time was 4 s, resistance change of Na ISM textile sensor and d) K ISM textile sensor in different buffer solutions can be found.

the resistance was then calculated. First, the *I–V* curve of the ISM textile sensors was performed in DI water, and this resistance value served as a reference data point for the analysis of the resistance changes in different buffer solutions (1, 5, 10, and 50 mM). Subsequently, the ISM textile sensors were submerged in buffer solutions (pH = 7) with concentrations ranging from low to high (1–50 mM) to obtain the resistance.

Figure 5b shows the *I–V* characterization of the Na ISM textile sensors after being submerged in various sodium buffer solutions for 10 s. The *I–V* curves were measured three times, and they exhibited a linear relationship between current and voltage with minimal error bars ($n = 3$). Figure 5c presents the resistance change obtained from the *I–V* characterization, indicating the detection of ions using the Na ISM textile sensors. The red curve displays the resistance change of Na ISM textile sensors when immersed in varying concentrations of sodium buffer solution. In contrast, the black curve represents the resistance change of textile sensors without ISM, which were submersed in different concentrations of sodium buffer solution. Lastly, the blue curve shows the resistance change of the Na ISM textile sensors submerged in various concentrations of potassium buffer solution. As indicated by the red curve in Figure 5c, the Na ISM textile sensors exhibited a high sensitivity (1182.67 Ohm $\log^{-1}$ (mM)) toward sodium ions over a concentration range from 1 to 50 mM. Compared to the textile sensors without ISM, the textile sensors covered with the Na ISM persist in exhibiting a high sensitivity toward the sodium ion detection. The results indicate that enough sodium ions are permeating through the ISM onto the PEDOT:PSS, even in the presence of the Na ISM. As a result, the conductivity of PEDOT:PSS shows strong variations, leading to a change in resistance of the textile sensors. Additionally, the Na ISM textile sensors displayed a minimal resistance change when submerged in different potassium buffer solutions, providing the evidence of their high selectivity against potassium ions.

As shown in Figure 5d, the resistance changes of K ISM textile sensors indicate their strong ability to detect ions. The red curve represents the resistance changes of the K ISM textile sensors when immersed in varying concentrations of potassium buffer solution. Meanwhile, the blue curve displays the resistance change of K ISM textile sensors submerged in various concentrations of sodium buffer solution. Those K ISM textile sensors also exhibited a high sensitivity (768.64 Ohm $\log^{-1}$ (mM)) toward potassium ions within the concentration range of 1–50 mM. Moreover, the K ISM textile sensors demonstrated only a slight change in resistance in sodium buffer solutions, indicating their high selectivity to sodium ions. These results proved that the PEDOT:PSS-based textile sensors with an integrated ISM can be used as a highly sensitive sensor for the desired ion with a high selectivity against undesired ions.

4. Conclusion

We present a simple fabrication method for preparing PEDOT:PSS-based textile sensors by immersing cotton yarn into PEDOT:PSS solutions for various times. Our fabrication technique could potentially be scaled up to produce large quantities of textile sensors. Moreover, the textile sensors displayed stable sensor responses and flexible behavior. Our results indicate that the textile sensors maintained their stability over a period of 5 d, and the resistance of the sensors was independent on bending angles. With the integration of Na or K ISMs, the textile sensors can be utilized as highly sensitive sensors to detect the desired ion concentration range of 1–50 mM, while maintaining a highly selective detection against undesired ions. The electrochemical characterization of the textile sensors provided the evidence that resistance changes of the textile sensors were accomplished through ion diffusion into the PEDOT:PSS, even without a third electrode as in OECTs. Our proof-of-concept highlights the potential of utilizing a two-terminal electrode configuration to achieve the electrical response and ion detection. In contrast to OECTs, our sensors with a two-terminal electrode configuration also simplify the read-out process for the sensor readout.

In the future, the fabrication method for ISM textile sensors could be enhanced by submerging the sensors in membrane solution for variable durations, enabling more precise control over the fabrication parameters. For ion detection, optimization of the ISM, including the compositions and thickness, will be carried out to further investigate their influence on the sensitivity and selectivity of the ion detection. Moreover, other ISMs, such as those for calcium and chloride, could also be integrated on the textile sensors to enable the detection of calcium ion and chloride ion. Additionally, the entire fiber-based sensor platform shows great potential for the integration with wearable and flexible sensors. However, few perspectives need to be considered: first of all, metal wires should be substituted with materials that can be easily integrated into e-textile through the weaving or sewing processes. Next, investigating textile sensors in complex environments is essential to guarantee their reliability and performance in real-world situations, including fluctuating temperatures, humidity, and stress. Then, it is crucial to upload the inherent characteristics of textile sensors, such as their flexibility to accommodate body movements, resistance to multiple washing cycles, and biocompatibility for sustained use. These textile sensors also show their significance across a variety of applications including sweat monitoring, environmental sensing, and the development of smart clothing.

Acknowledgements

Financial support for this project came from the program for the promotion of Industrial Collective Research (IGF) in the format CORNET. In the project Hybrid-E-Tattoo (351EN/2), the authors develop combined on-skin wearable sensors and smart textiles. C.L. acknowledges financial support by the Chinese Scholarship Council (201906280065). Additional financial support came from the RWTH Aachen University.

Open Access funding enabled and organized by Projekt DEAL.

Conflicts of Interest

The authors declare no conflict of interest.

Data Availability Statement

The data that support the findings of this study are available from the corresponding author upon reasonable request.

Keywords

ion detection, ion-selective membranes, PEDOT:PSS, smart clothing, textile sensors

Received: January 17, 2024
Revised: March 28, 2024
Published online:

[1] S. Cho, T. Chang, T. Yu, C. H. Lee, *Biosensors* **2022**, *12*, 222.
[2] M. R. Islam, S. Afroj, K. S. Novoselov, N. Karim, *Adv. Sci.* **2022**, *9*, 2203856.
[3] N. Coppedè, G. Tarabella, M. Villani, D. Calestani, S. Iannotta, A. Zappettini, *J. Mater. Chem. B* **2014**, *2*, 5620.
[4] Y. Zhao, Q. Zhai, D. Dong, T. An, S. Gong, Q. Shi, W. Cheng, *Anal. Chem.* **2019**, *91*, 6569.
[5] A. Piper, I. Ö. Månsson, S. Khaliliazar, R. Landin, M. M. Hamedial, *Biosens. Bioelectron.* **2021**, *194*, 113604.
[6] A. Ortiz-Conde, F. J. García Sánchez, J. J. Liou, A. Cerdeira, M. Estrada, Y. Yue, *Microelectron. Reliab.* **2002**, *42*, 583.
[7] L. Possanzini, F. Decataldo, F. Mariani, I. Gualandi, M. Tessarolo, E. Scavetta, B. Fraboni, *Sci. Rep.* **2020**, *10*, 17180.
[8] N. Coppedè, M. Giannetto, M. Villani, V. Lucchini, E. Battista, M. Careri, A. Zappettini, *Org. Electron.* **2020**, *78*, 105579.
[9] L. Manjakkal, W. Dang, N. Yogeswaran, R. Dahiya, *Biosensors* **2019**, *9*, 14.
[10] W. Gao, S. Emaminejad, H. Y. Y. Nyein, S. Challa, K. Chen, A. Peck, H. M. Fahad, H. Ota, H. Shiraki, D. Kiriya, D. H. Lien, G. A. Brooks, R. W. Davis, A. Javey, *Nature* **2016**, *529*, 509.
[11] Y. Yang, W. Gao, *Chem. Soc. Rev.* **2019**, *48*, 1465.
[12] S. T. Keene, D. Fogarty, R. Cooke, C. D. Casadevall, A. Salleo, O. Parlak, *Adv. Healthcare Mater.* **2019**, *8*, 1901321.
[13] A. P. Jones, L. M. C. Webb, A. O. Anderson, E. J. Leonardo, A. Rot, *J. Leukocyte Biol.* **1995**, *57*, 434.
[14] D. H. Choi, J. S. Kim, G. R. Cutting, P. C. Searson, *Anal. Chem.* **2016**, *88*, 12241.
[15] M. Chung, G. Fortunato, N. Radacsi, Chung, M., G. Fortunato, N. Radacsi, *J. R. Soc. Interface* **2019**, *16*, 20190217.
[16] A. J. Bandodkar, W. J. Jeang, R. Ghaffari, J. A. Rogers, *Annu. Rev. Anal. Chem.* **2019**, *12*, 061318.
[17] B. Schazmann, D. Morris, C. Slater, S. Beirne, C. Fay, R. Reuveny, N. Moyna, D. Diamond, *Anal. Methods* **2010**, *2*, 342.
[18] A. J. Bandodkar, D. Molinnus, O. Mirza, T. Guinovart, J. R. Windmiller, G. V. Ramírez, F. J. Andrade, M. J. Schöning, J. Wang, *Biosens. Bioelectron.* **2014**, *54*, 603.
[19] D. B. Speedy, T. D. Noakes, C. Schneider, *Emerg. Med.* **2001**, *13*, 17.
[20] W. Gao, H. Y. Y. Nyein, Z. Shahpar, L. C. Tai, E. Wu, M. Bariya, H. Ota, H. M. Fahad, K. Chen, A. Javey, *IEEE Commun. Mag.* **2016**, *1*, 1011.
[21] D. Kinnamon, R. Ghanta, K. C. Lin, S. Muthukumar, S. P. Kinnamon, *Sci. Rep.* **2017**, *7*, 13312.
[22] J. Kim, A. S. Campbell, J. Wang, *Talanta* **2018**. *177*, 163.
[23] M. Beauchamp, L. C. Lands, L. C. Lands, *Pediatr. Pulmonol.* **2005**, *39*, 507.
[24] A. A. Llobregat, I. Jeerapan, A. Bandodkar, L. Vidal, A. Canals, J. Wang, E. Morallón, Abellan-Llobregat, *Biosens. Bioelectron.* **2017**, *91*, 885.
[25] L. Groenendaal, F. Jonas, D. Freitag, H. Pielartzik, J. R. Reynolds, *Adv. Mater.* **2000**, *12*, 481.
[26] F. Hempel, J. K. Y. Law, T. C. Nguyen, R. Lanche, A. Susloparova, X. T. Vu, S. Ingebrandt, *Biosens. Bioelectron.* **2021**, *180*, 113101.
[27] Y. Liang, F. Brings, V. Maybeck, S. Ingebrandt, B. Wolfrum, A. Pich, A. Offenhäusser, D. Mayer, *Adv. Funct. Mater.*, **2019**, *29*, 1902085.
[28] C. Liao, C. Mak, M. Zhang, H. L. W. Chan, F. Yan, *Adv. Mater.* **2015**, *27*, 676.
[29] A. Campana, T. Cramer, D. Simon, M. Berggren, F. Biscarini, *Adv. Mater.* **2014**, *26*, 3874.
[30] D. Khodagholy, J. N. Gelinas, T. Thesen, W. Doyle, O. Devinsky, G. G. Malliaras, G. Buzsáki, *Nat. Neurosci.* **2015**, *18*, 310.
[31] M. Tintelott, T. Kremers, S. Ingebrandt, V. Pachauri, X. T. Vu, *Sensors* **2022**, *22*, 2999.
[32] S. Han, N. U. H. Alvi, L. Granlöf, H. Granberg, M. Berggren, S. Fabiano, X. Crispin, *Adv. Sci.* **2019**, *6*, 1802128.
[33] M. Serafini, F. Mariani, I. Gualandi, F. Decataldo, L. Possanzini, M. Tessarolo, B. Fraboni, D. Tonelli, E. Scavetta, Serafini, *Sensors* **2021**, *21*, 7905.
[34] J. Zhang, Q. Zhou, J. Cao, W. Wu, H. Zhang, Y. Shi, Q. Mao, H. Ma, *Cellulose* **2021**, *28*, 3123.
[35] I. Gualandi, M. Tessarolo, F. Mariani, L. Possanzini, E. Scavetta, B. Fraboni, *Polymers* **2021**, *13*, 894.
[36] G. Tarabella, M. Villani, D. Calestani, R. Mosca, S. Iannotta, A. Zappettini, N. Coppedè, *J. Mater. Chem.* **2012**, *22*, 23830.
[37] L. Possanzini, *II Nuovo Cimento C* **2021**, *44*, 1.
[38] A. Yang, Y. Li, C. Yang, Y. Fu, N. Wang, L. Li, F. Yan, *Adv. Mater.* **2018**, *30*, 1800051.
[39] M. Tintelott, T. Kremers, A. Mernitz, S. Ingebrandt, V. Pachauri, X. T. Vu, U. Schnakenberg, *Electroanalysis* **2023**, *35*, e202200332.
[40] Y. Li, B. Cui, S. Zhang, B. Li, J. Li, S. Liu, Q. Zhao, *Small* **2022**, *18*, 2107413.
[41] M. Ghittorelli, L. Lingstedt, P. Romele, N. I. Crăciun, Z. M. K. Vajna, P. W. M. Blom, F. Torricelli, *Nat. Commun.* **2018**, *9*, 1441.
[42] A. Cadogan, Z. Gao, A. Lewenstam, A. Ivaska, *Anal. Chem.* **1992**, *164*, 2496.
[43] M. Sessolo, J. Rivnay, E. Bandiello, G. G. Malliaras, H. J. Bolink, *Adv. Mater.* **2014**, *26*, 4803.
[44] D. Khodagholy, T. Doublet, P. Quilichini, M. Gurfinkel, P. Leleux, A. Ghestem, E. Ismailova, T. Herve´, S. Sanaur, C. Bernard, G. G. Malliaras, *Nat. Commun.* **2013**, *4*, 1575.
[45] S. Han, S. Yamamoto, A. G. Polyravas, G. G. Malliaras, *Adv. Mater.* **2020**, *32*, 2004790.
[46] S. Demuru, B. P. Kunnel, D. Briand, S. Demuru, B. P. Kunnel, D. Briand, *Adv. Mater. Technol.* **2020**, *5*, 2000328.
[47] A. Fick, *J. Membr. Sci.* **1995**, *100*, 33.
[48] F. Wang, S. Kumari, U. D. Schiller, F. Wang, S. Kumari, U. D. Schiller, *Phys. Rev. Mater.* **2020**, *4*, 083804.
[49] A. B. Nyoni, D. Brook, *J. Text. Inst.* **2006**, *97*, 119.